Paweł ORKISZ*

LABORATORY STAND FOR TESTING THE ACTIVE VIBRATION CONTROL SYSTEM WITH ENERGY REGENERATION

SUMMARY

The paper describes an active vibration control system for a structure of two degrees of freedom. The system comprises two elastically connected bodies moving along vertical guides. The system structure is additionally provided with two electrodynamical linear motors working in energy regeneration and active vibration reduction subsystems. The combination of these subsystems with a special control system creates a self-powered vibration reduction system, allowing active vibration control of the second body using the energy from the motion of the first body, which was regenerated and stored in capacitors.

Keywords: *active vibration control system, energy regeneration, measuring systems, self-powered systems*

STANOWISKO DO TESTOWANIA AKTYWNYCH UKŁADÓW REDUKCJI DRGAŃ Z REGENERACJĄ ENERGII

W pracy przedstawiono aktywny system redukcji drgań układu o dwóch stopniach swobody. Układ składa się z dwóch brył połączonych sprężyście, poruszających się wzdłuż prowadnic. Zastosowano dwa elektrodynamiczne silniki linowe pracujące w układzie odzyskiwania energii oraz w układzie aktywnej wibroizolacji Połączenie obydwu układów systemem sterowania umożliwiło budowę samozasilającego się układu wibroizolacji. Pozwala on na aktywną redukcję drgań drugiej bryły przy wykorzystaniu odzyskanej i zmagazynowanie w kondensatorach energii pochodzącej z drgań bryły pierwszej.

Słowa kluczowe: *aktywny układ redukcji drgań, odzysk energii, systemy pomiarowe, samozasilające się układy*

1. INTRODUCTION

Taking into consideration the advances in technology and in current ergonomics, many devices designed at the present time should be equipped with vibration control systems. Active vibration reduction systems are, for example, used in suspension systems (Fodor *et al.* 1993). The control algorithms for active vibration reduction systems are realized by using devices powered by external sources of energy. At the same time mechanical vibration energy is converted into heat in dampers. This paper aims to develop a system facilitating the storage of vibration energy and its reuse in the active vibration control system (Nakano *et al.* 2003).

Figure 1 presents a diagram of the two degrees of freedom system under analysis. The system is excited kinematically by a vibrating platform. A system with two degrees

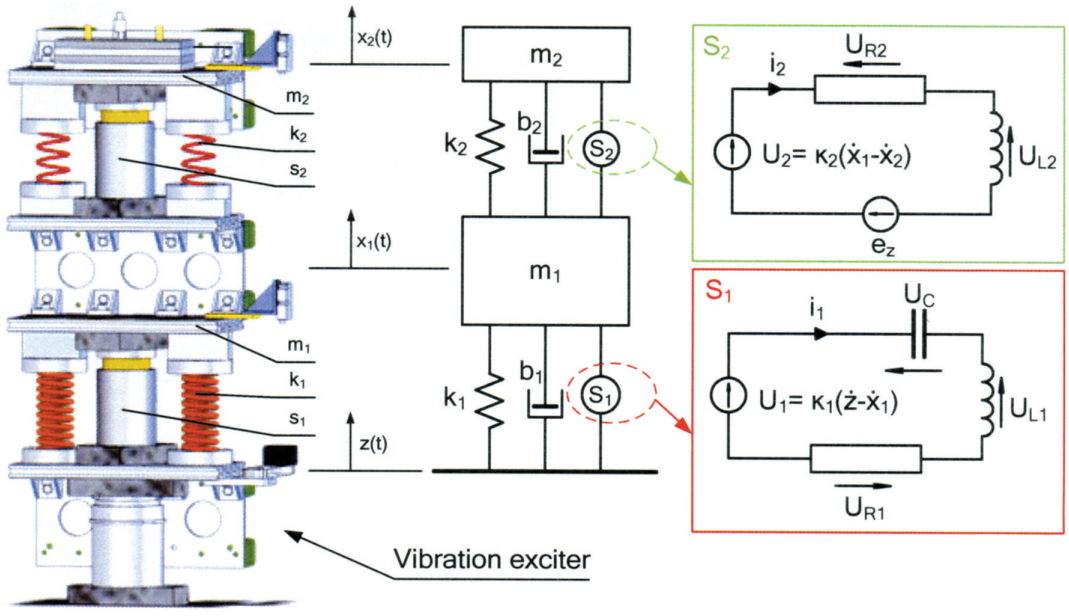

Fig. 1. System diagram

* AGH University of Science and Technology, Faculty of Mechanical Engineering and Robotics, Department of Process-Control, al. A. Mickiewicza 30, 30-059 Krakow, Poland; Orkisz@agh.edu.pl

of freedom was assumed. Bodies with m_1 and m_2 mass are connected by springs with stiffness constants k_1, k_2 and viscous dampers with damping coefficients b_1, b_2. In addition, the system is provided with linear motors to serve as active components (Kowal *et al.* 2008). The system is kinematically excited by a moving platform. The location of the motor for the energy regeneration process and the one performing the active control results from the operational diagram of the assumed system. The lower motor is located closer to the source of vibration. This is convenient in terms of the quantity of energy being recuperated. The upper motor acts on the body that models the subsystem being protected from vibrations. Such a configuration is rather schematic and it aims to assign functions to individual subsystems. From the perspective of physical phenomena, mechanical energy is transferred to both the lower and upper motors. Both motors may operate as generators. Some of the electricity converted from the mechanical energy and stored in a capacitor or a battery is used in the upper motor circuit, with the aim to force the possible reception of mechanical energy from the object being controlled.

2. MATHEMATICAL MODEL OF A VIBRATION SYSTEM WITH TWO DEGREES OF FREEDOM

The formulation of the state equations follows the analysis of the mechanical and electrical parts (Snamina *et al.* 2009). The assumption, at this stage of the study, is that the lower and upper motor circuits are independent, as shown in Figure 1. It was assumed that the motors are ideal devices, operating without losses. The mechanical power is therefore equal to the electrical one. The constitutive equations for the motors take the following form:

$$\begin{cases} u_1 = \kappa_1 \left(\dot{z} - \dot{x}_1 \right) \\ S_1 = \kappa_1 i_1 \end{cases} \qquad \begin{cases} u_2 = \kappa_2 \left(\dot{x}_1 - \dot{x}_2 \right) \\ S_2 = \kappa_2 i_2 \end{cases} \tag{1}$$

where $\kappa_1 \kappa_2$ are motor parameters, and S_1, S_2 the forces with which the motors act on the mechanical subsystems.

The state variables included in the vector $\left[x_1 \;\; v_1 \;\; x_2 \;\; v_2 \;\; q_1 \; i_1 \;\; i_2 \right]^T$ were assumed for the description of the system. They refer, respectively, to the displacement and velocity of the lower body, the displacement and velocity of the upper body, the capacitor charge, and the current in the lower and upper motor circuits. The input values are the platform displacement and source voltage in the upper motor circuit. After application of the basic equations describing the motion of the mechanical systems, the equations describing the electric circuits and the constitutive equations for the electrical linear motors, the state equations for the electro-mechanical system will take the form:

$$\begin{cases} \dfrac{dx_1}{dt} = v_1 \\ \dfrac{dv_1}{dt} = \dfrac{1}{m_1}\left[-\left(k_1 + k_2\right) x_1 - \left(b_1 + b_2\right) v_1 + k_2 x_2 + \right. \\ \left. + b_2 v_2 + \kappa_1 i_1 - \kappa_2 i_2 \right] + \dfrac{1}{m_1}\left[k_1 z + b_1 \dot{z} \right] \\ \dfrac{dx_2}{dt} = v_2 \\ \dfrac{dv_2}{dt} = \dfrac{1}{m_2}\left[k_2 x_1 + b_2 v_1 - k_2 x_2 - b_2 v_2 + \kappa_2 i_2 \right] \\ \dfrac{dq_1}{dt} = i_1 \\ \dfrac{di_1}{dt} = \dfrac{1}{L_1}\left[-\kappa_1 v_1 - \dfrac{1}{C} q_1 - R_1 i_1 \right] + \dfrac{\kappa_1}{L_1} \dot{z} \\ \dfrac{di_2}{dt} = \dfrac{1}{L_2}\left[\kappa_2 v_1 - \kappa_2 v_2 - R_2 i_2 \right] + \dfrac{1}{L_2} e_z \end{cases} \tag{2}$$

The voltages related to inductances in both circuits, at the frequencies under study, are negligible. The omission of the systems' inductances simplifies the electro-mechanical system description. Thus the state vector can be reduced to the form: $\left[x_1 \;\; v_1 \;\; x_2 \;\; v_2 \;\; q_1 \right]^T$. The state equations will then take the following form:

$$\begin{cases} \dfrac{dx_1}{dt} = v_1 \\ \dfrac{dv_1}{dt} = \dfrac{1}{m_1}\left[-\left(k_1 + k_2\right) x_1 - \left(b_1 + b_2 + \dfrac{\kappa_1^2}{R_1} + \dfrac{\kappa_2^2}{R_2} \right) v_1 + k_2 x_2 \right] + \\ + \dfrac{1}{m_1}\left[\left(b_2 + \dfrac{\kappa_2^2}{R_2} \right) v_2 - \dfrac{\kappa_1}{R_1 C} q_1 + k_1 z + \left(b_1 + \dfrac{\kappa_1^2}{R_1} \right) \dot{z} - \dfrac{\kappa_2}{R_2} e_z \right] \\ \dfrac{dx_2}{dt} = v_2 \\ \dfrac{dv_2}{dt} = \dfrac{1}{m_2}\left[k_2 x_1 + \left(b_2 + \dfrac{\kappa_2^2}{R_2} \right) v_1 - k_2 x_2 - \left(b_2 + \dfrac{\kappa_2^2}{R_2} \right) v_2 \right] + \\ + \dfrac{\kappa_2}{m_2 R_2} e_z \\ \dfrac{dq_1}{dt} = \dfrac{1}{R_1}\left[-\kappa_1 v_1 - \dfrac{1}{C} q_1 \right] + \dfrac{\kappa_1}{R_1} \dot{z} \end{cases} \tag{3}$$

3. MATHEMATICAL MODEL OF THE ENERGY REGENERATIVE SYSTEM

To allow capacitor charging, a rectifier system must be introduced to the electric circuit of the lower motor. This is due to the oscillating character of the state variables describing the system. It is possible to apply half wave or full wave rectification. Half wave rectification will result in a slower charging of the capacitor, yet could be a part of the system generating an asymmetric damping force, which is often assumed in, for example, suspension systems. State equations in which the capacitor charging process is included during system motion, take the following form:

$$\begin{cases} \dfrac{dx_1}{dt} = v_1 \\ \dfrac{dv_1}{dt} = \dfrac{1}{m_1}\left[-(k_1+k_2)x_1 - \left(b_1+b_2+\dfrac{\kappa_1^2}{R_1}\right)v_1\right] + \\ + \dfrac{1}{m_1}\left[k_2x_2 + b_2v_2 - \dfrac{\kappa_1}{R_1C}q_1 + k_1z + \left(b_1+\dfrac{\kappa_1^2}{R_1}\right)\dot{z}\right] \\ \dfrac{dx_2}{dt} = v_2 \\ \dfrac{dv_2}{dt} = \dfrac{1}{m_2}\left[k_2x_1 + b_2v_1 - k_2x_2 - b_2v_2\right] \\ \dfrac{dq_1}{dt} = i_1 \end{cases} \tag{4}$$

The i_1 charging current assumed in the calculations for half-wave rectification can be determined from the equation:

$$i_1 = \begin{cases} \dfrac{1}{R_1}\left[-\kappa_1 v_1 - \dfrac{1}{C}q_1\right] + \dfrac{\kappa_1}{R_1}\dot{z} & \text{for } \dfrac{1}{R_1}\left[-\kappa_1 v_1 - \dfrac{1}{C}q_1\right] + \dfrac{\kappa_1}{R_1}\dot{z} > 0 \\ 0 & \text{for } \dfrac{1}{R_1}\left[-\kappa_1 v_1 - \dfrac{1}{C}q_1\right] + \dfrac{\kappa_1}{R_1}\dot{z} \le 0 \end{cases} \tag{5}$$

For full-wave rectification, the charging current can be described as:

$$i_1 = \left|\frac{1}{R_1}\left[-\kappa_1 v_1 - \frac{1}{C}q_1\right] + \frac{\kappa_1}{R_1}\dot{z}\right| \tag{6}$$

4. MATHEMATICAL MODEL OF THE ACTIVE ENERGY DISSIPATION SYSTEM

The control algorithm model discussed herein is based on an energy analysis of the system, and it aims to achieve a potentially large amount of energy dissipation in the upper circuit. The 'energy flow' in the system is relatively simple and involves the conversion of mechanical energy into electrical, and the transformation of electrical energy into heat (Joule Lenz heat). In a viscous damper the mechanical energy is transformed directly into heat. The selection of an appropriate control algorithm comes down to transferring the largest amount of mechanical energy into electrical one, which is then turned into heat. Assuming that the motor is an ideal device, the power of "the mechanical side" is the same as that on "the electrical side". The mechanical energy dissipation criterion at a given moment is based on the fact that the power introduced to the electric circuit is positive. The executing device operates as a generator. This corresponds to the condition in which, the generator force acting on the body is directed opposite to the relative velocity of bodies. The energy is consumed from the mechanical system. According to the above analysis, the simplest control of voltage source placed in the circuit involves switching its polarisation so that the electromotive force of the source adds to the generator voltage.

The concept of forced mechanical energy dissipation by means of an active system may be executed in various ways. The simplest control formula is obtained by assuming the following force description:

$$S_2 = \frac{\kappa_2^2}{R_2}(v_1 - v_2) + S_{op}\,sign(v_1 - v_2) \tag{7}$$

where S_{op} is the parameter of the control system. The acting force has two components; the first takes the form of viscous resistance and the second takes that of Coulomb friction force. The form of the first component is the same as there is no control source placed in the circuit. The source being controlled is intended to achieve the additional force described by the second component. Current intensity corresponding to the force described by equation (7) can be determined from the formula:

$$i_2 = \frac{\kappa_2}{R_2}(v_1 - v_2) + \frac{S_{op}}{\kappa_2}sign(v_1 - v_2) = i_{20} + i_{2z} \tag{8}$$

Similarly as for the force $S_{2,}$ the formula describing current intensity, $i_{2,}$ has two components; the first, marked as i_{20} is responsible for generating the force of viscous resistance, and the second, marked as $i_{2z,}$, is responsible for generating the Coulomb friction resistance force. Taking into account the constitutive equations for the executing device and the current intensity descriptions, it can be stated that:

$$i_{20} = \frac{u_2}{R_2} \tag{9}$$

Ultimately, the voltage of the controlled source can be calculated with the Kirchhoff's second law. It takes the form of:

$$e_z = \frac{S_{op}R_2}{\kappa_2}sign(v_2 - v_1) = e_{op}\,sign(u_2) = R_2 i_{2z} \tag{10}$$

The expression (10) describing the voltage of the source being controlled was provided in three forms, using predefined values. The second form, which underlines the ease with which the control can be executed, deserves attention. The only value needed to execute the algorithm related to the current system status is the easily measurable voltage in the execution device, and, more precisely, only its sign. The source voltage marked e_{op} is arbitrary and the force acting on the mechanical subsystem can be calculated on the basis of its value, using a simple equation:

$$S_{op} = \frac{e_{op}\kappa_2}{R_2} \tag{11}$$

5. MATHEMATICAL MODEL OF THE ACTIVE VIBRATION CONTROL SYSTEM WITH ENERGY REGENERATION

The vibration reduction system combined with the energy regeneration system, forming a self-powered vibration control system. The proposed system stores energy regenerated from the movement of the lower body in a capacitor, assuming full-wave rectification. The energy stored in the capacitor is used for dissipation of energy from the mechanical subsystem with the aid of the upper motor. In this case, the capacitor serves as the source. To allow control with the vibration reduction system, the electrical circuits of both motors are connected to a switching system, allowing changes in the source polarisation. Taking into consideration the mathematical models already discussed, the final form of the state equations for the energy regenerative system and the controlled voltage source in the vibration reduction system can be presented as follows:

$$\begin{cases}
\dfrac{dx_1}{dt} = v_1 \\
\dfrac{dv_1}{dt} = \dfrac{1}{m_1}\left[-(k_1+k_2)x_1 - \left(b_1+b_2+\dfrac{\kappa_1^2}{R_1}+\dfrac{\kappa_2^2}{R_2}\right)v_1\right] + \\
+\dfrac{1}{m_1}\left[k_2x_2 + \left(b_2+\dfrac{\kappa_2^2}{R_2}\right)v_2 - \dfrac{\kappa_1}{R_1C}q_1\right] + \\
+\dfrac{1}{m_1}\left[k_1z + \left(b_1+\dfrac{\kappa_1^2}{R_1}\right)\dot{z} - \dfrac{\kappa_2}{R_2}e_{op}sign\left[\kappa_2(v_1-v_2)\right]\right] \\
\dfrac{dx_2}{dt} = v_2 \\
\dfrac{dv_2}{dt} = \dfrac{1}{m_2}\left[k_2x_1 + \left(b_2+\dfrac{\kappa_2^2}{R_2}\right)v_1 - k_2x_2 - \left(b_2+\dfrac{\kappa_2^2}{R_2}\right)v_2\right] + \\
+\dfrac{\kappa_2}{m_2R_2}e_{op}sign\left[\kappa_2(v_1-v_2)\right] \\
\dfrac{dq_1}{dt} = \left|\dfrac{1}{R_1}\left[-\kappa_1v_1 - \dfrac{1}{C}q_1\right] + \dfrac{\kappa_1}{R_1}\dot{z}\right|
\end{cases} \tag{12}$$

The following parameters are used in calculations m_1 = 5.4 kg, m_2 = 4.0 kg, k_1 = 12.5·10^3 N/m, b_1 = 60 Ns/m, k_2 = 6.66·10^3 N/m, b_2 = 20 Ns/m, κ_1 = 21.35 N/A, κ_2 = 21.36 Vs/m, R_1 = 2.4 Ω, R_2 = 2.4 Ω, C = 58 F. The simulation tests of active vibration control system began with the charging the capacitor to reach a voltage value of e. The calculations were performed assuming a harmonic forcing of variable frequency and constant amplitude. Amplitude-frequency characteristics of the upper body displacement are shown in Figure 2.

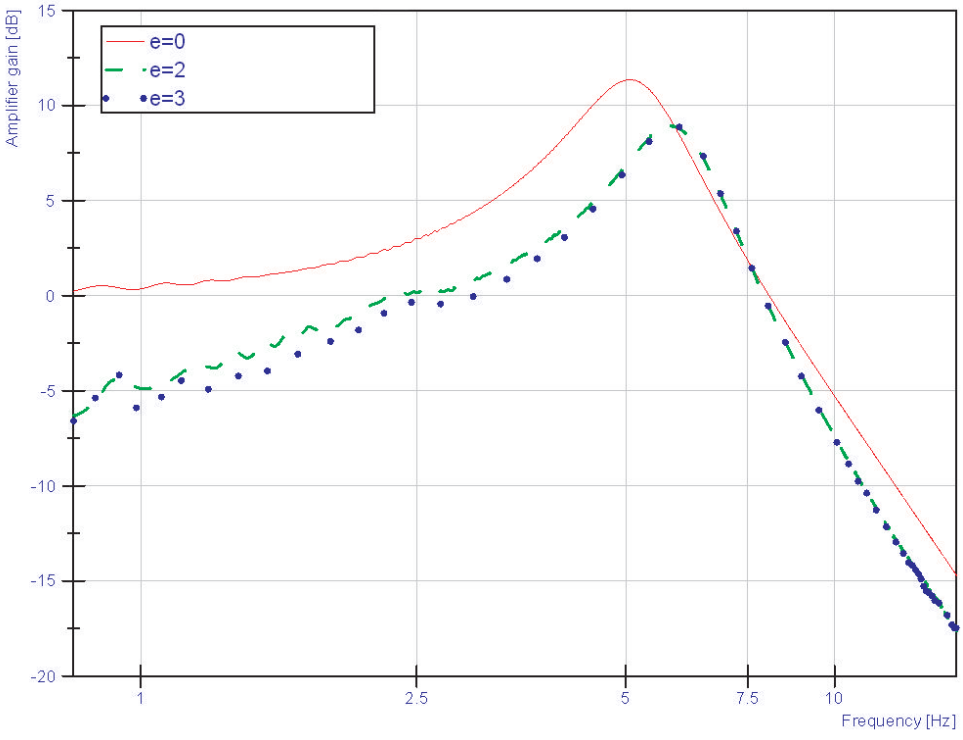

Fig. 2. Amplitude-frequency characteristics of the upper body displacement

6. THE STRUCTURE OF THE LABORATORY STAND FOR TESTING VIBRATION CONTROL SYSTEMS USING THE LINEAR MOTORS

In order to verify the mathematical model the active vibration control system was designed. The stand was divided into three main parts: testing, measuring and control. The stand configuration is shown in Figure 3.

The testing section of the stand, shown in Figure 4, comprises a frame structure (1), to which the components of the vibration reduction system are mounted, as well as the converters and conditioning system parts. Taking into consideration the forcing system, three platforms on linear bearings were designed (3, 8 12), between which the components of the tested vibration control system, such as the LA25 linear motors (6, 10) and the spring sets (9, 5), are mounted. The first platform, acting as an electromagnetic

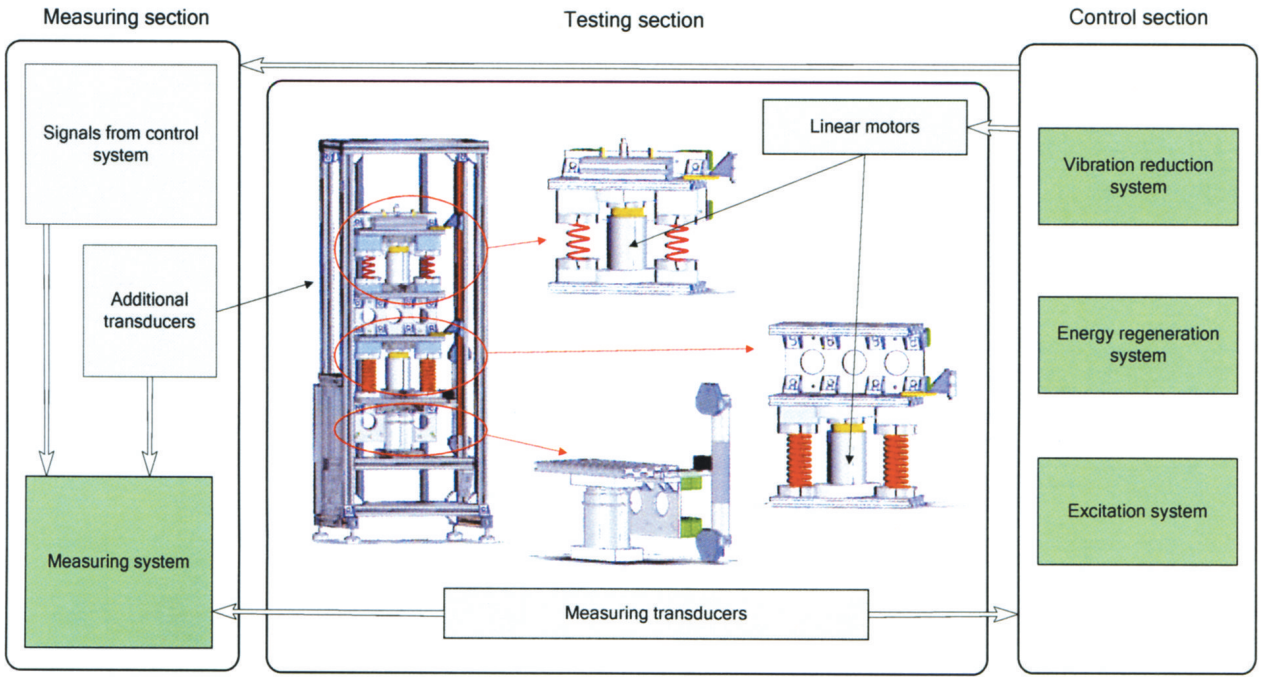

Fig. 3. The scheme of Laboratory stand

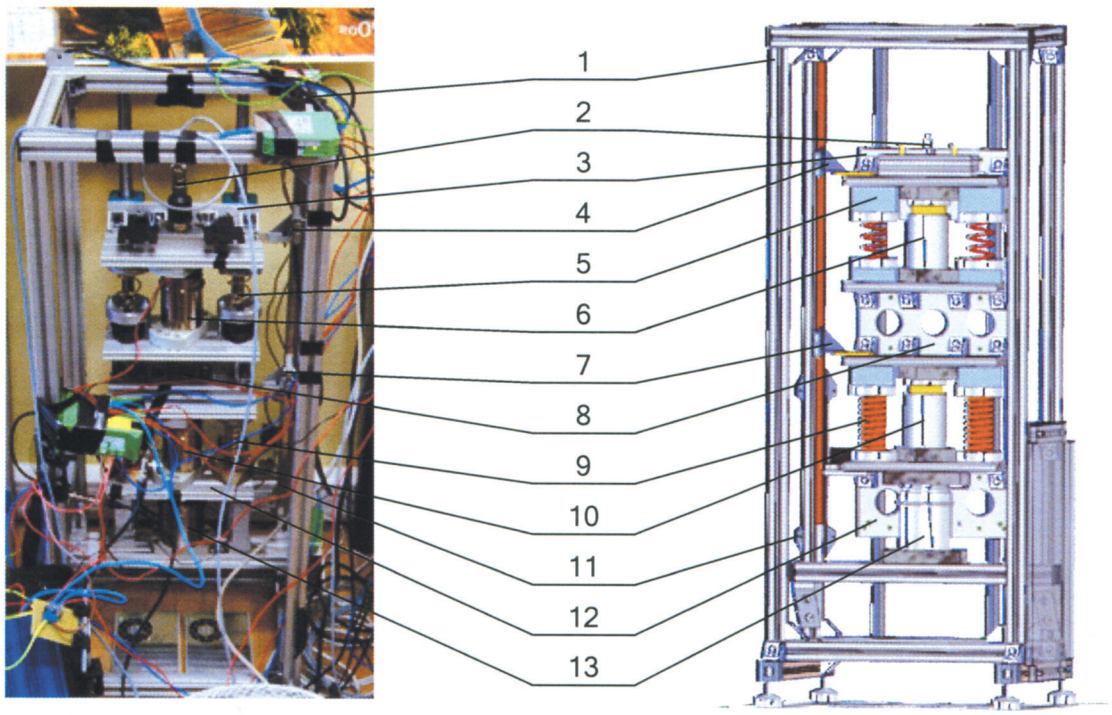

Fig. 4. The testing section of the laboratory workstation

vibration generator, is provided with the LA30 linear electrodynamical motor (13), and the magnetostrictive displacement transmitter (11). The stand is additionally provided with incremental heads, which are the linear encoders (4, 7) and piezoelectric acceleration transducers (2), for example, part 2 shown in Figure 4. The displacement transmitters were selected with the aim of achieving a high measuring resolution of 0.01 mm for platforms 3 and 8, and 0.1 mm for platform 12.

The complex structure of the control and measuring system made it necessary to create two parts, for control and measurement, respectively. The measuring part comprises a NI cDAQ 9172 controller with three NI 9215 measuring cards. Each of the cards allows the simultaneous recording of four analogue channels with a resolution of 16 bits at a maximum range of ±10 V. The solution allows the measuring channels to be recorded and scaled and the results to be saved on a PC connected to the measuring unit (King 2008). The measuring transducers used permit the recording of the displacement and acceleration of individual platforms, the voltage in the capacitor charging system, the current intensities in the energy regeneration and energy dissipation circuits, and the static and dynamic forces. The solution also enables recording taking into consideration the synchronisation of the signals used in the control system, such as the set value and regulation deviation values. The measuring system is provided with a graphic interface which facilitates the viewing of the current measuring signals being recorded and the selection of the location for files.

To build the control part shown in Figure 5, an NI cRIO 9074 controller provided with a programmable array of logic gates FPGA was utilised. It is composed of a real-time processor connected with the FPGA module via a data-bus. The module manages a data rail with a connection terminal for I/O cards. The TCP/IP communication modules allow the data imaging and operation of remote control panels to be controlled and measured, bearing in mind the simultaneous input of variables from multiple independent network locations such as a PC, for example, or an operator panel. Archiving the control data is made possible by means of exchanging data streams with Ehternet or sharing pre-saved files with the FTP service.

The tests were carried out using the LabView programming environment. The controller programming is a multi-staged process. The first stage defines the structure of the I/O modules; the data exchange is arranged by reserving the appropriate memory blocks and the data exchange channels assigned to them. The next stage is the preparation and compilation of the program to be executed by the FPGA module. The final stage involves the preparation of a control program, which will be executed by the real-time processor. Those tasks requiring a constant sampling period, as well as safety-related tasks, were performed in the FPGA system. Such a solution makes the system operation independent of the software, as the control algorithms are executed at the hardware level.

The vibration reduction system was combined with the energy regeneration system and a self-powered vibration

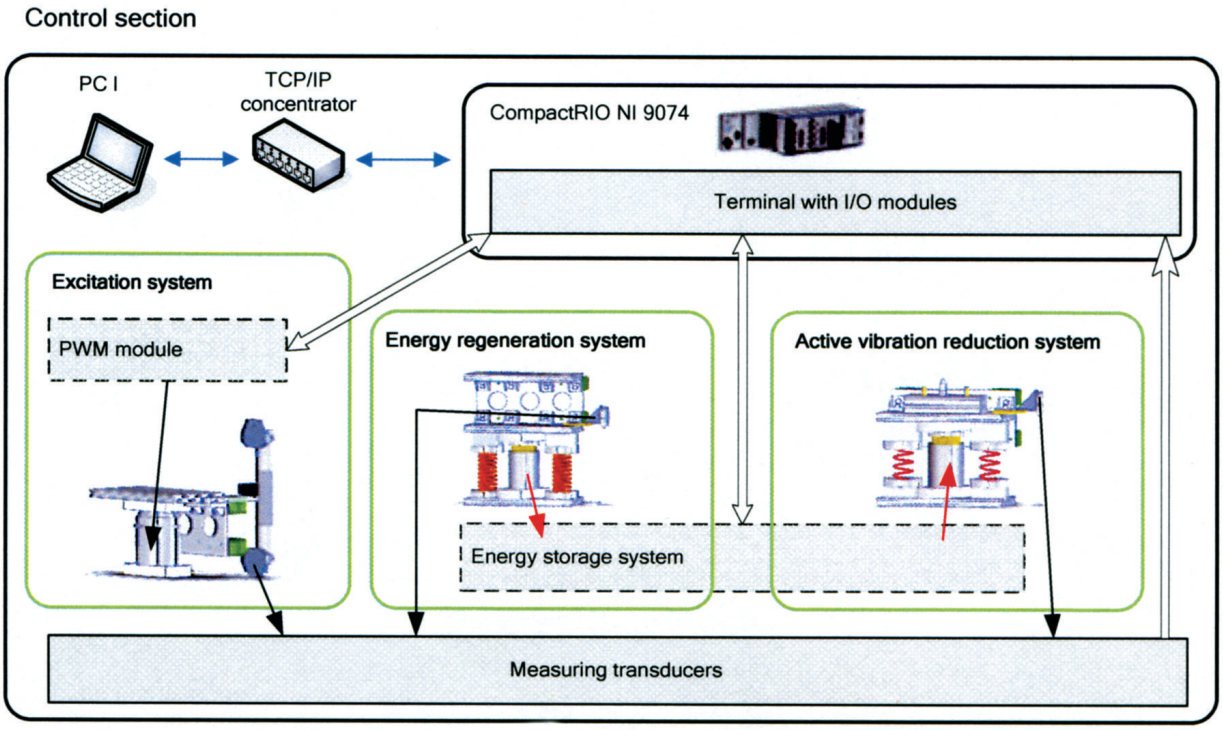

Fig. 5. Control system diagram

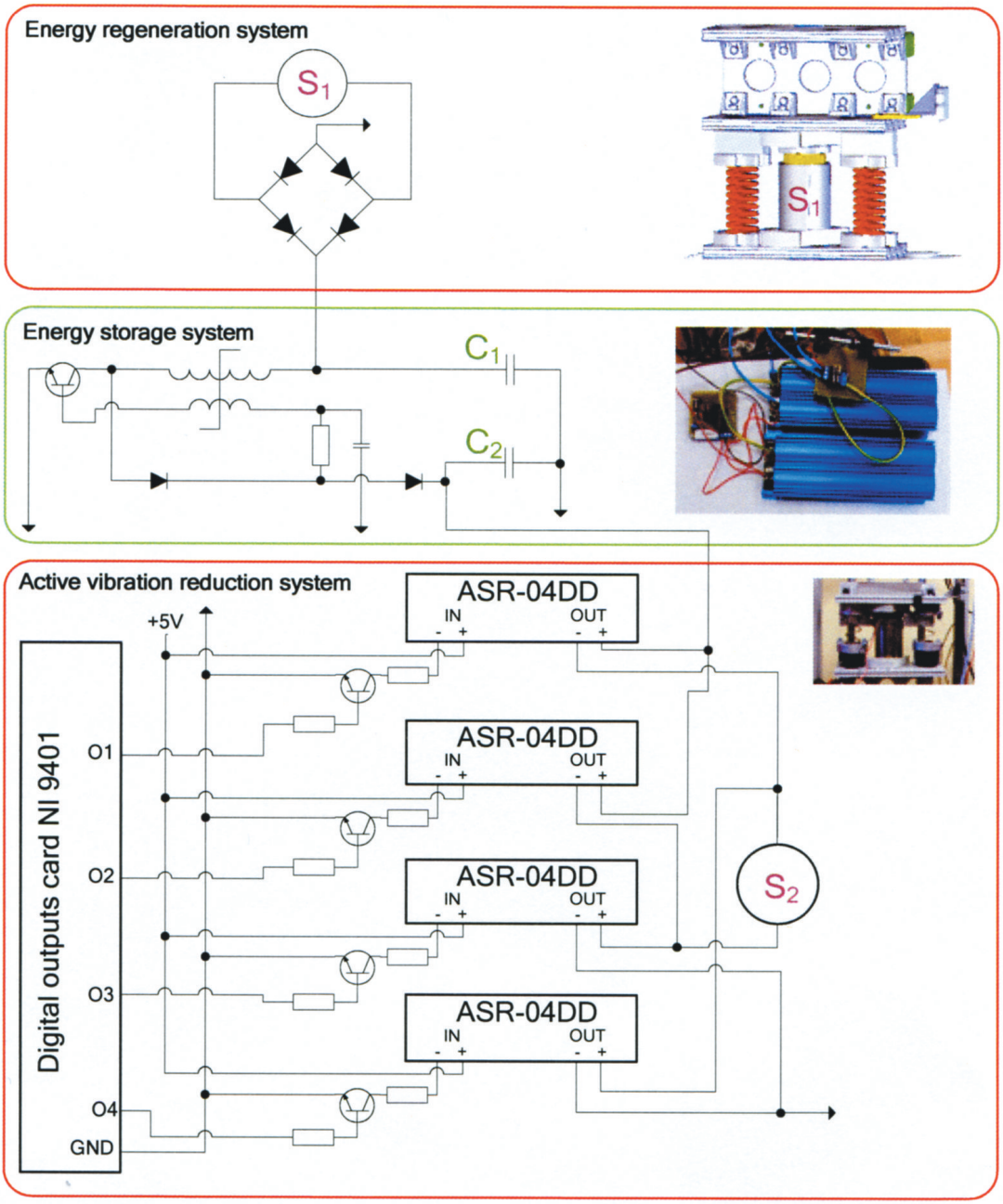

Fig. 6. Diagram of the active vibration reduction system with energy regeneration

control system was thus formed. Two 58F Maxwell ultra capacitors were used to supply the vibration control system and for the storage of energy. Figure 6 shows a diagram of the electrical system. Full-wave rectification was assumed for the charging system. The voltage of the first capacitor, C_1, is raised so that the maximum amount of energy can be stored in capacitor the C_2, which serves as the power supply source. An energy regeneration system prepared in this way was connected to the vibration reduction system with the aid of four relays in order to allow the switching of the source polarisation. Control of the vibration reduction system is carried out with digital outputs connected to the switching system.

7. LABORATORY TESTS OF THE VIBRATION CONTROL SYSTEM

The laboratory workstation allows the testing of an active vibration control system with energy regeneration in the frequency ranges present in practice, up to 20 Hz. The experiments were performed assuming harmonic forcing of variable frequency and constant amplitude. The main limitation of the active vibration control system is the high demand for external energy; the tests began with charging the C_2 capacitor to reach a voltage value of U_p. The results of the displacement measurements for body mass m_2 with anti-offset high-pass filter are presented as the amplitude-frequency characteristics in Figure 7.

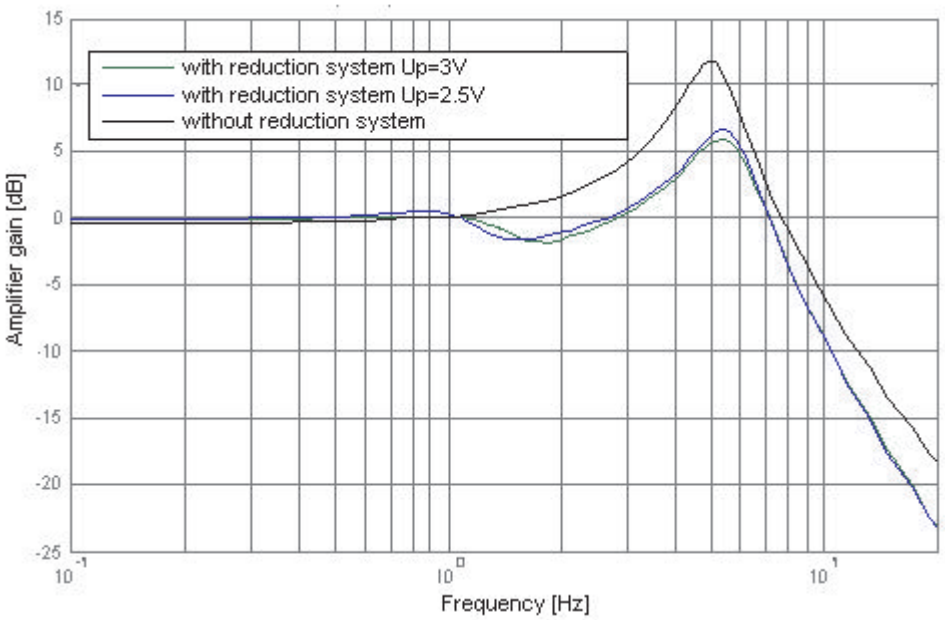

Fig. 7. Amplitude-frequency characteristics of the upper body displacement

8. SUMMARY

The laboratory workstation allows comprehensive tests to be carried out on experimental vibration control systems. Its main advantages are the measurement possibilities related to experiment repeatability, and the possibility of carrying out comprehensive testing of vibration reduction systems of varied structure. Due to relatively high passive damping the efficiency of the vibration control system presented in the paper cannot be significant. However, it should be noted that the algorithm presented here will always improve vibration control efficiency, regardless of the capacitor charge and the inner damping of the mechanical subsystem. In theory, it is possible to select such mechanical parameters for the system as to ensure that, for specific forcing signals, the energy stored will be equal to that consumed by the active vibration control system.

References

Fodor M., Redfield R. 1993, *The variable linear transmission for regenerative damping in vehicle suspension control*. Vehicle System Dynamics 22, 1–20.

Nakano K., Suda Y, Nakadai S. 2003, *Self-powered active vibration control using a single electric actuator*. Journal of Sound and Vibration, 260, 213–235.

King R. 2008, *Introduction Acquisition with LabVIEW*. McGraw-Hill.

Kowal J., Konieczny J., Orkisz P. 2008, *Zastosowanie elektromagnetycznego silnika liniowego do redukcji drgań mechanicznych*. Wydawnictwo Politechniki Krakowskiej.

Snamina J., Podsiadło A., Orkisz P. 2009, *Skyhook vibration control with energy regenerative system*. Mechanics, vol. 28.